Discovery of chromene compounds as inhibitors of PvdQ acylase of Pseudomonas aeruginosa

Vogel, Jan G T; Wibowo, Joko P; Fan, Hillina; Setroikromo, Rita; Wang, Kan; Dömling, Alexander; Dekker, Frank J; Quax, Wim J

IMPORTANT NOTE: You are advised to consult the publisher's version (publisher's PDF) if you wish to cite from it. Please check the document version below.

Document Version
Publisher's PDF, also known as Version of record

[Link to publication in University of Groningen/UMCG research database](#)

Original article

Discovery of chromene compounds as inhibitors of PvdQ acylase of *Pseudomonas aeruginosa*

Jan G.T. Vogel [a], Joko P. Wibowo [a, b], Hillina Fan [a], Rita Setroikromo [a], Kan Wang [c], Alexander Dömling [c], Frank J. Dekker [a], Wim J. Quax [a, *]

[a] Department of Chemical and Pharmaceutical Biology, Groningen Research Institute of Pharmacy, University of Groningen, Antonius Deusinglaan 1, Groningen, 9713, AV, the Netherlands
[b] Faculty of Pharmacy, University of Muhammadiyah Banjarmasin, Jl. Gubernur Syarkawi, Barito Kuala, 70582, Indonesia
[c] Department of Drug Design, Groningen Research Institute of Pharmacy, University of Groningen, Antonius Deusinglaan 1, Groningen, 9713, AV, the Netherlands

ARTICLE INFO

ABSTRACT

The acquisition of iron is a crucial mechanism for the survival of pathogenic bacteria such as *Pseudomonas aeruginosa* in eukaryotic hosts. The key iron chelator in this organism is the siderophore pyoverdine, which was shown to be crucial for iron homeostasis. Pyoverdine is a non-ribosomal peptide with several maturation steps in the cytoplasm and others in the periplasmatic space. A key enzyme for its maturation is the acylase PvdQ. The inhibition of PvdQ stops the maturation of pyoverdine causing a significant imbalance in the iron homeostasis and hence can negatively influence the survival of *P. aeruginosa*. In this work, we successfully synthesized chromene-derived inhibitory molecules targeting PvdQ in a low micromolar range. In silico modeling as well as kinetic evaluations of the inhibitors suggest a competitive inhibition of the PvdQ function. Further, we evaluated the inhibitor *in vivo* on *P. aeruginosa* cells and report a dose-dependent reduction of pyoverdine formation. The compound also showed a protecting effect in a *Galleria mellonella* infection model.

© 2022 The Author(s). Published by Elsevier Masson SAS on behalf of Institut Pasteur. This is an open access article under the CC BY license (http://creativecommons.org/licenses/by/4.0/).

Pseudomonas aeruginosa is known as a facultative pathogen that poses a low health risk to healthy individuals, but a high risk to immunocompromised hosts [1]. In cystic fibrosis patients, *P. aeruginosa* is a predominant cause of morbidity and mortality due to its ability to form biofilms resulting in hard-to-treat chronic infections [2]. Additionally *P. aeruginosa* is recognized as a multidrug-resistant pathogen in clinical settings and was catalogized as a priority pathogen by the "World Health Organization" in 2017 [3]. Therefore, new strategies and therapies to combat the infections caused by this bacterium are urgently needed.

Iron is one of the most abundant elements on earth, however, it is predominantly found in its Fe^{3+} oxidative state which makes it unavailable for biological processes. Hence organisms have evolved iron acquisition systems as well as strategies to strictly maintain iron homeostasis [4]. *P. aeruginosa* is taking up iron from the surrounding environment amongst others with the help of the potent siderophore pyoverdine [5]. Especially in the context of infectious diseases, the competition for iron plays an important role on both sides in host−microbe interactions. In the case of *P. aeruginosa* infections, the iron acquisition is even macroscopically visible, since pyoverdine and pyocyanin give the bacterium its characteristic green-blue phenotype. Already in the middle of the 19th-century physicians described a greenish discoloration of wound badges [6].

The biosynthesis and activity of pyoverdine have been known since 1985 [7]. Several cytoplasmic and periplasmic enzymes are involved in its production. In the periplasmatic space alone six different enzymes are involved in the maturation of pyoverdine [8,9]. One of these enzymes is the acylase PvdQ, which is cleaving the acyl chain from acetyl ferribactin which is a precursor form of pyoverdine [10]. Next, two enzymes, PvdP and PvdO continue the process via multiple oxidative cyclizations of ferribactin, resulting in the fluorescent pyoverdine product [11]. At the final step of the biosynthesis, the pyoverdine is modified by PvdN [12] or PtaA [13]. The maturated pyoverdine is exported via various transport systems into the environment. Once excreted pyoverdine is considered a common good, which means that it is available to all surrounding cells [14]. A PvdQ knock-out mutant has been reported showing reduced excretion of virulence factors, including pyoverdine production [15]. In response to this fact, several studies have reported

* Corresponding author.
E-mail address: w.j.quax@rug.nl (W.J. Quax).

their findings on the inhibitors of PvdQ as a novel strategy against *P. aeruginosa* infections. A study on N-alkylboronic acid inhibitors enabled resolution of a crystal structure, which provides insight in determinants of ligand specificity in the quorum-quenching and siderophore biosynthetic enzyme PvdQ [16]. However, molecules with unsaturated aliphatic chains usually lack specificity due to hydrophobic interactions. A subsequent study enabled identification of a biaryl nitrile compound that competitively inhibits PvdQ acylase. The mode of binding was confirmed by a crystal structure of the PvdQ acylase bound to the inhibitor [17].

Following the encouraging results mentioned above, we tried to find a new class of inhibitor for PvdQ acylase based on a slightly different scaffold as compared to previous works. In this work, we report novel inhibitors of PvdQ, identified from a library of 81 compounds based on a chromene scaffold. The screening of the compound library on the inhibition of the acylase activity of PvdQ resulted in 4 inhibitors showing low micromolar potency. Among these inhibitors, compound **4d** showed the most potent inhibition activity (IC$_{50}$ = 4.70 ± 0.51 μM), and kinetic experiments revealed that compound **4d** acted as a competitive inhibitor. In silico modelling helped to generate hypothetical binding poses, which are in accordance with the biological data. Biological evaluation of the compound also showed the potency in an *in vivo* pyoverdine production assay as well as in a *Galleria mellonella* infection model.

1. Materials and methods

1.1. Chemistry general

Unless noted, all solvents and reagents were purchased from Abcr GmbH, Acros, AK Scientific, Fluorochem, and Sigma—Aldrich and were used without further purification. Thin-layer chromatography was performed on precoated silica gel GF$_{254}$ (Merck, Germany). Nuclear magnetic resonance spectra were recorded in Bruker Avance 500 or 600 Spectrometer ^{1}H NMR (500 MHz, 600 MHz), ^{13}C NMR (126 MHz, 151 MHz). The chemical shifts for ^{1}H NMR were reported as values and coupling constant in hertz (Hz). The following abbreviations were used for spin multiplicity: s = singlet, br. s = broad singlet, d = doublet, t = triplet, q = quartet, qu = quintet, dd = double of doublets, dd = double of doublet of doublets, m = multiplet. The chemical shifts for ^{13}C NMR were reported in ppm related to the solvent peak. Flash chromatography was performed in a Reveleris® X2 flash Chromatography system using Grace® Reveleris Silica flash cartridges (12 g). Mass spectra were measured on a Waters Investigator Supercritical Fluid Chromatography with 3100 MS Detector (ESI) using a solvent system of methanol and CO$_2$ on Viridis silica gel column (4.6 × 250 mm, 5 μm particle size). High-resolution mass spectra were recorded using an LTQ-Orbitrap-XL (Thermo Scientific, the Netherlands) at a resolution of 60,000@*m/z* 400.

1.2. General procedure to synthesize the chromene compounds

Cyanoacetamide (1.0 mmol) and sodium ethoxide (0.2 mmol) were added into a stirred solution of 2H-chromen-2-one (1.0 mmol) in dry ethanol (5 mL). The stirring was continued at room temperature for 24 h. The precipitant was filtered and washed with cold ethanol (2 x 5 mL), yielding the final products (35—81%) without further purification.

1.3. Expression and purification of PvdQ

PvdQ enzyme was overexpressed and purified according to the previous report [18]. Briefly, the enzyme was purified in three steps using an ÄktaPure system. Firstly, the harvested cell pellet was resuspended in 3 times (w/v) lysis buffer (50 mM TRIS—HCl pH = 8.5, 2 mM EDTA). Subsequently, the suspension was lysed by sonication, and the cell debris was removed by centrifugation at 18.000 rpm for 1 h at 4 °C. The first purification step consists of an ion exchange HiTrap Q Fast Flow column separating the proteins by charge. The resulting lysate is subsequently separated based on hydrophobicity. A HiTrap Sepharose column (GE Healthcare, Germany) was used to obtain the enzyme where it was previously equilibrated with 50 mM Tris—HCl pH = 8.5, 2 mM EDTA, and 700 mM ammonium sulfate. PvdQ was eluted at the end of the 0—700 mM gradient concentration of ammonium sulfate. Lastly, a HiLoad Superdex 75 16/160 gel filtration column (GE Healthcare, Germany) was used to purify PvdQ by collecting the major peak; afterward, the enzyme was concentrated to 1 mg/mL. The purified enzyme was aliquoted to 200 μL, snap-frozen in liquid nitrogen, and stored in −80 °C until further use.

1.4. Enzymatic assay of PvdQ

The enzymatic activity of PvdQ against 4-nitrophenyl laurate (pNP laurate) was performed based on a method by Drake and Gulick with a minor modification [19]. The liberation of p-nitrophenol was monitored at A$_{405}$ in a SPECTROstar® Omega microplate reader (BMG Labtech, Germany) continuously in transparent 96 well plates (VWR International, US). In our experiments, the substrate was not sufficiently dissolved by following the previous report [19]. Therefore, we first dissolved the substrate in 100% 2-hydroxypropane and subsequently diluted it in the reaction mix to reach the final concentration of 10% 2-hydroxypropane, 27.5 mM Tris pH 8.0, 0.6 μM PvdQ, with the substrate concentration 1—100 μM. We collected the initial acylase rate data (up to 4 min of measurement) on the different concentrations of the substrate. Afterward, the K$_m$ and V$_{max}$ were calculated using GraphPad Prism 5.0 based on the Michaelis—Menten equation. The reactions were performed in three independent experiments.

1.5. Screening of chromene library

Initial screening of the inhibition of chromene compounds on the acylase activity of PvdQ was conducted using the same method as mentioned above. The final concentration of each component was 10% 2-hydroxypropane, 27.5 mM Tris pH 8.0, 0.6 μM PvdQ, pNP laurate 25 μM. The chromene compounds were dissolved in DMSO, resulting in the final concentration of 25 μM in DMSO 5%. The experiments were conducted three times independently.

The compounds with the highes potency in the screening were subjected to IC50 determination. The same format was used for IC50 determination in which assay enzyme activity in presence of inhibitor concentrations ranging between 0 and 25 μM. The experiments were conducted in three independent series. Calculation with the obtained data were done using the GraphPad Prism 5.0. Software.

1.6. Kinetic assay of PvdQ with compound 4d

To investigate the mechanism of compound **4d** inhibition on the PvdQ acylase activity, we conducted kinetic assays using compound **4d** in the condition mentioned above. Briefly, three different concentrations of compound **4d** around its IC$_{50}$ value were used. The obtained data were plotted as 1/velocity (1/V) vs. 1/substrate concentration (1/[S]) on the Lineweaver—Burk plot. K$_m$ and V$_{max}$ were also determined based on the same data set. All experiments were performed three times independently.

1.7. Molecular docking study of compound 4d on PvdQ

A molecular docking study was performed to study the binding between compound **4d** and PvdQ. The crystal structure of PvdQ (PDB ID = 4WKV) was downloaded from the PDB database. The 2D structure of compound **4d** was drawn in MarvinSketch 18.3, 2018, ChemAxon (http://www.chemaxon.com), then converted into a 3D structure, geometrically optimized, energy-minimized, and saved as a.mol2 file using Avogadro [20]. The molecular docking study following the standard protocol was performed using Autodock Vina [21] running on UCSF Chimera [22] by setting the grid box at the active site of PvdQ. The docking results were visualized using Pymol [23] for the 3D depiction and LigPlot+ [24] for the 2D depiction.

1.8. Pyoverdine cell-based assay

The assay was performed in a white flat bottom 96 well plate with clear buttom from Thermo Scientific. Pyoverdine was measured at its absorbance maximum of 405 nm. Measurements were performed in a BMG Fluorostar plate reader and normalized by the OD $_{600nm}$ of the bacterial cultures. The starting OD of PAO1, as well as PAO1ΔpvdQ in this assay, was set to OD $_{600nm}$ 0.02. The bacteria were incubated for 10 h in the BMG Fluorostar plate reader at 37 °C, orbital shaking 300 rpm between measurements. Each condition was measured in quintuplicate and every data point represents the average of 5 measurements.

1.9. Galleria mellonella *killing assay*

The *G. mellonella* larvae used in all experiments were purchased in the shop "Frits Kuipers" - Groningen (the Netherlands). The larvae were stored at 18 °C in the dark and used within 3 days after purchase. Each experiment consisted of a group of 10 individual larvae. The groups were randomly selected with a bodyweight of 250−350 mg. *P aeruginosa* PAO1 was cultured in LB medium until an $OD_{600\ nm}$ of 0.1 and harvested by centrifugation and washed once with sterile PBS to achieve 10^3 colony-forming units per milliliter (CFU/ml). 10 μl of the bacterial suspension were injected into the hemocoel of each larva via the last left proleg (HumaPen Luxura; Lilly Nederland). Bacterial colony counts on LB agar were used to confirm all inocula. After injection, the larvae were incubated at 37 °C. The number of dead larvae was scored daily for 4 days. The larvae were considered dead when they displayed no movement in response to touch.

2. Results

2.1. Synthesis of the compound library

A compound library with a focus on the chromene scaffold was synthesized using a method as described in the previous report [25]. This library consists of a chromene core with substitution of an amino group in 2-position and a fused piperidinodione ring. As mentioned before that previous works have successfully discovered new inhibitors of PvdQ acylase based on the alkyl boronic acid [16] and biaryl nitrile [17], therefore, in this work we expand the exploration of a new inhibitor based on the chromene scaffold by the variation of the side chain. We developed the method by Rosati et al. using a number of different cyanoacetamides and substituted 2H-chromenes. Then, we designed and synthesized a diverse library utilizing aromatic and aliphatic substituents, heterocycles, hydrogen acceptors, and donors. Furthermore, we also improved the solubility of some compounds by introducing morpholino substituents. The reactions were conducted under a

mild condition with different cyanoacetamides in good yields. All 81 compounds were analyzed by ^{1}H NMR and LC-MS to identify their structure and the most relevant ones are shown in Supplementary Information.
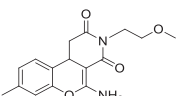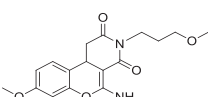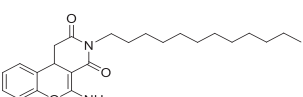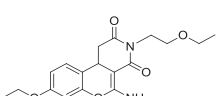
2.2. Enzymatic assay of PvdQ

By optimizing the enzymatic reaction condition, we did not only solve the solubility problem of the substrate, but we were also able to more accurately determine its kinetic parameters (K_m = 24.35 μM, V_{max} = 0.0130 A_{405}/min). Following the optimization of the enzymatic reaction condition, an initial screening of the compound library of chromene scaffold was performed to investigate their inhibition activity on PvdQ. The compounds were tested using a spectrophotometer based on the absorbance of para nitrophenol (pNP) at 405 nm. The reaction was conducted using a single concentration of pNP laurate (25 μM) and each compound (25 μM) from a DMSO stock. The final concentration of DMSO in the reaction, which did not influence the enzymatic activity, was at a maximum of 5%. The results (Tables S1−S6) show that some compounds have >50% inhibition and for these hit compounds, the IC_{50}s were calculated (Table 1). This revealed that some compounds showed inhibition of the acylase activity of PvdQ at a low micromolar range.

Looking at the chemical structures of these hit compounds it appeared that substitution on the R is giving various effects on the inhibition activity. In general, bulky substituents, such as morpholines, furans, thiophenes, and naphthalenes, give a low effect on the inhibition. On the other hand, aliphatic chain substitution showed much better inhibition.

A methoxyethyl substitution at the aliphatic chain (10a) showed mild inhibition (IC_{50} = 33.82 ± 3.20 μM). Extending the chain with a methoxypropyl (17c) showed slightly improved inhibitory activity (IC_{50} = 19.53 ± 2.53 μM). A variation on the position of oxygenatom on the same chain with an ethoxyethyl (10e) resulted in stronger inhibitory activity (IC_{50} = 9.20 ± 1.80 μM). These results indicate that the length of the chain and the position of atom O influence the activity of the compounds. Furthermore, the substitution with a C12 aliphatic chain (**4d**) showed the strongest activity (IC_{50} = 4.70 ± 0.51 μM) among the compounds in this library.

Table 1
The IC_{50} of the most potent compounds on the inhibition of PvdQ.

Compound	Structure	Inhibition Activity at 25 μM (%)	IC_{50} ± SD (μM)
10a		53	33.82 ± 3.20
17c		56	19.50 ± 2.53
4d		74	4.70 ± 0.51
10e		54	9.20 ± 1.80

SD = standard deviation of three independent experiments.

2.3. Evaluation of kinetic parameters

To investigate the mechanism of inhibition of the inhibitor, we conducted a kinetic evaluation on compound **4d**. The Michaelis−Menten equation at different concentrations of compound **4d** demonstrates a typical competitive inhibition. Whereas the K_m values changed, the V_{max} remained the same at different concentrations of the inhibitor. In support of the Michaelis−Menten equation, the Lineweaver−Burk plots on the same data set further confirm the competitive inhibition activity of compound **4d** (Fig. 1).

The result is correlated with the binding mode of a previously identified compound 1-octylboronic acid [26]. It means by sharing the same substituent, compound **4d** has the same mechanism of inhibition as the previously reported inhibitor. It also confirms that the aliphatic "tail" is an important group to occupy the hydrophobic pocket resulting in a competitive type of inhibition of PvdQ.

2.4. Molecular docking results corroborate a competitive inhibition of compound 4d

To gain more insight into the binding between the inhibitor and PvdQ, a molecular docking study was performed. The molecular docking result showed that compound **4d** fits the substrate pocket of the PvdQ enzyme (Fig. 2A). The inhibitor shows a strong hydrophobic interaction with the residues on the cavity of the substrate pocket. This interaction is stabilized by hydrogen bonding to Ser217 and Asn485 (Fig. 2B). Apparently, these two residues are important to facilitate the binding of the ligand to the enzyme. Interestingly a similar interaction between ligand and enzyme involving these residues was reported previously [26].

2.5. Pyoverdine production is reduced upon the addition of compound 4d

As a next step, we evaluated the impact of the inhibitor in an *in vivo* pyoverdine production assay. It could be shown that the addition of compound **4d** results in a dose-dependent reduction of the production of pyoverdine in comparison with the wild-type strain PAO1 (Fig. 3). The compound was added in a concentration range from 10 μM to 250 μM, as a benchmark measurement, we used PAO1 Δ*pvdQ*.

2.6. Compound 4d shows a higher survival rate in a G. mellonella infection model

Pyoverdine is considered one of *P. aeruginosa's* key virulence determinant [27]. The impact of pyoverdine on the course of a *P. aeruginosa* infection was evaluated in a *G. mellonella* infection

model. This model is widely used to assess the virulence of bacteria like *P. aeruginosa*. Furthermore, *G. mellonella* exhibits a complex innate immune system making it a valuable infection model [28]. The infection was induced with 10 CFU of *P. aeruginosa* PAO1 and the inhibitor **4d** was added at a concentration of 250 μM since that showed the highest amount of inhibition of pyoverdine. As postulated, it is visible that the survival rate of the treated individuals is significantly higher than the untreated group (Fig. 4). The PvdQ negative strain is not able to produce pyoverdine and also showed an increased survival rate in comparison to the untreated group (10 CFU) which is on the same level as the group treated with compound **4d**. The compound control group, which was injected only with sterile compound **4d** showed that there was no cytotoxic effect detectable in this model. In conclusion, the inhibitor seems to have a beneficial effect on the course of a PAO1 induced infection in a *G. mellonella* infection model.

3. Discussion

In the fight against MDR bacteria novel compounds for new targets are very important to provide new drugs in the future. The attenuation of virulence factors with small molecules offers a novel angle on treating bacterial infections. It is important to note that the inhibitor as it is presented in this work does not actively kill *P. aeruginosa* cells but impairs their ability to survive in the host environment. This is also due to a tightly regulated iron homeostasis of the host [29].

We could observe that the supplementation of pyoverdine could recover the virulence in the *pvdQ* deficient mutant (Fig. S4). Furthermore, the addition of PVD has an influence on the *G. mellonella* larvae on its own as shown in Fig. S5. The clearance of the infection is proposed to be done by the host immune system [30].

The compound screening revealed four potential inhibitors with compound **4d** being the most promising since it showed the strongest inhibitory activity. The compound's substitution of a C12 carbon chain mimics the natural substrate, namely the carbon chain of PVDiq. In Fig. 2, the superimposition between the docking result and PvdQ bound to PvdIq [31] showed the aliphatic chain of the inhibitor overlay with the aliphatic tail of the substrate occupying the active pocket. In an *in vivo P. aeruginosa* cell assay, a high concentration of the inhibitor is necessary to inhibit pyoverdine production.

The inhibition of PvdQ happens in the periplasmic space which has the advantage that the inhibitor does not need to cross into the cytoplasm to reach its target. Therefore, a compound with low hydrophobicity such as compound **4d** has to be able to reach the target site in the periplasm. In silico modeling predicts the binding
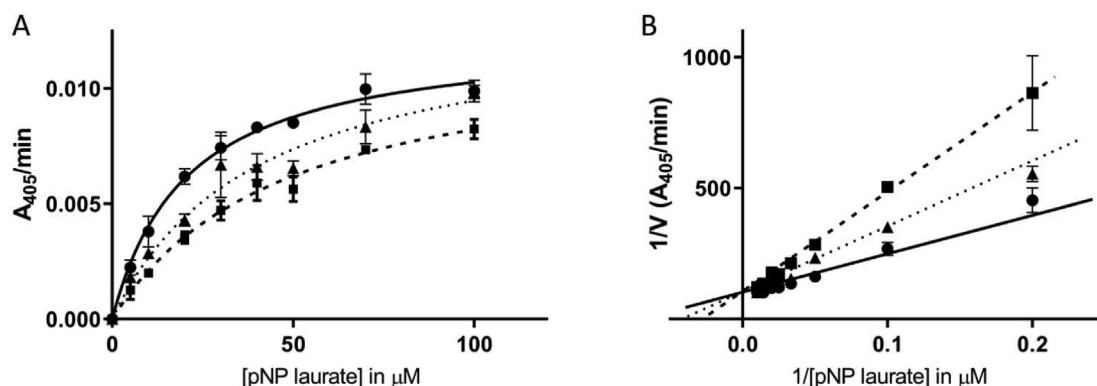

Fig. 1. Kinetic evaluation of compound 4d. (A) Michaelis−Menten graph, (B) Lineweaver−Burk plots, the concentration of compound **4d** are ● = 0 μM, ▲ = 2.5 μM, ■ = 5 μM.
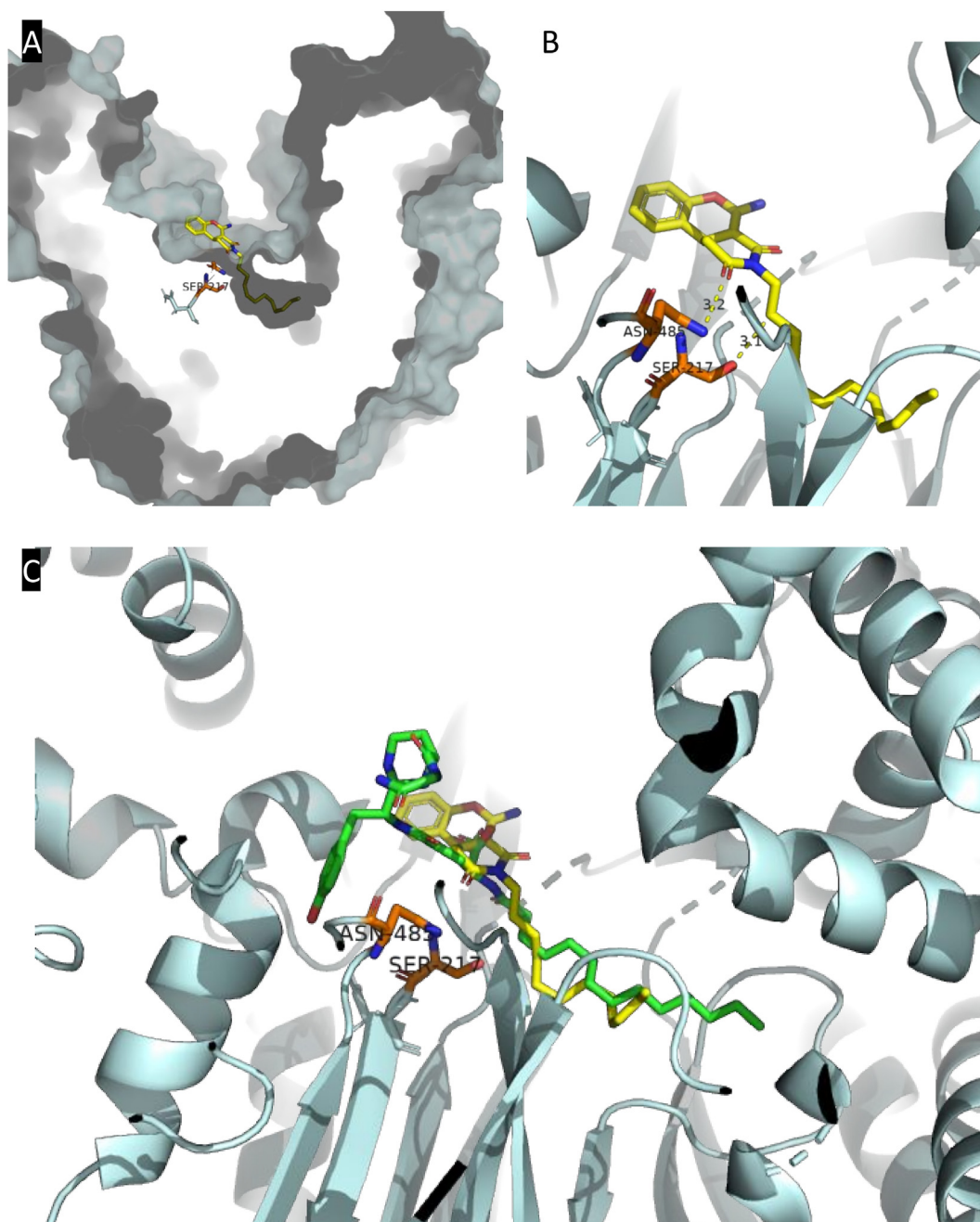
Fig. 2. The predictive binding mode of compound **4d** on the hydrophobic pocket of PvdQ. (A) The aliphatic "tail" fits the cavity of the hydrophobic pocket while the chromene "head" is exposed to the solvent, (B) a close up view of compound 4d (yellow) located in the active pocket forming hydrogen bond with Asn485 and Ser217 (orange), (C) superimposition between PvdIq (green) (PDB ID = 4UBK) and compound 4d (yellow) as shown both are located in the active site of PvdQ where the aliphatic "tail" of each compound overlap each other in the active site pocket.

mode of compound **4d**. It shows that the compound's aliphatic carbon chain seems to fit precisely in the hydrophobic pocket of PvdQ.

However, this long aliphatic tail and is still suboptimal with respect to its solubility. In its current state the compound is not ready to be marketed as a drug. Nevertheless, linear aliphatic chains have a high conformational flexibility, which enables them to interact with a variety of hydrophobic surfaces thus limiting their selectivity. Further development of these compounds along the same principles as found in the previous reports [16,17] holds promise to enhance both selectivity and potency, which will be

the next step to provide suitable lead compounds for drug discovery.

Further, the addition of compound **4d** to a *P. aeruginosa* culture clearly showed a dose-dependent reduction of the pyoverdine formation in the cell-based assay. The highest concentration of 250 μM compound **4d** shows a significant reduction of pyoverdine compared to the wild-type production. A comparison with the Δ*pvdQ* mutant shows that the inhibitor does not completely inhibit pyoverdine production, however, due to the aliphatic chain the compound has limited solubility and we could not increase the concentration further. We estimated the LogP value of compound
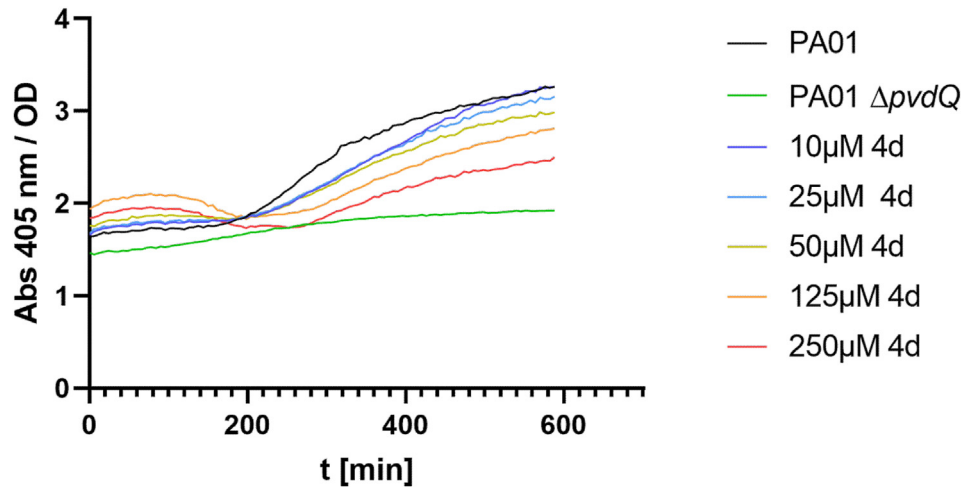
Fig. 3. Pyoverdine production and inhibition. The production of pyoverdine was assessed spectrophotometrically at the absorption maximum of 405 nm and normalized by the optical density of the culture. Compound 4d was tested in concentrations of 250 μM, 125 μM, 50 μM, 25 μM and 10 μM. Upon addition of inhibitor 4d we can observe a dose dependent reduction of the PVD production. The green line describes the ΔpvdQ mutant of PAO1. Each condition was measured in quintuplicate and every data point represents the average of 5 measurements.
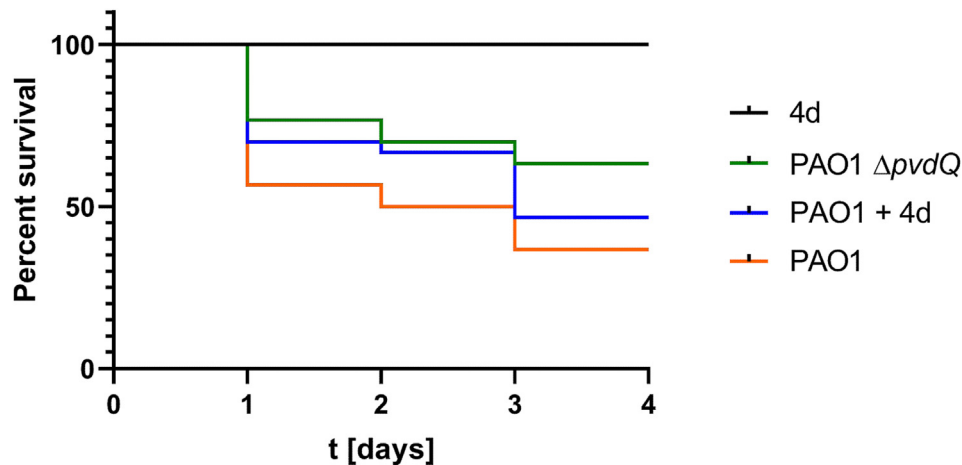

Fig. 4. The addition of 250 μM PvdQ inhibitor 4d (blue line) shows a significantly higher survival rate than individuals only challenged with 10 CFU PAO1 (orange line). Especially in the earlier stages of the infection after the first and second day, we could observe that the survival rates of the ΔpvdQ strain and the wild-type strain combined with the inhibitor are more similar then compared to the survival rate of the untreated group (orange line). The experiments were performed in triplicate, comparison of the survival curves was performed with a Log-rank (Mantel–Cox) test in the GraphPad Prism software. The number of animals per group in each experiment; n = 10.

4d using an online tool (https://www.molinspiration.com/cgi-bin/properties). The value is greater than 5 indicating a high hydrophobicity. This can explain the high concentrations needed in the cell-based pyoverdine assay to achieve the inhibition of pyoverdine production.

The same concentration of **4d** (250 μM), was also applied within the inoculum of *P. aeruginosa* in the *G. mellonella* infection model upon injection. Notably, the final concentration in the larvae is considerably lower than in the cell-based assay. Here we could observe a higher survival rate of the treated larvae in comparison to the untreated group. Both treated individuals, as well as individuals challenged with the ΔpvdQ knock-out mutant, showed a comparable survival rate. Taking this into account we see an effect of the inhibitor in a PAO1-based cell assay as well as in a *G. mellonella* infection model. Finally, a combination with antibiotics could result in a wholesome approach of inhibiting iron acquisition as well as actively killing *P. aeruginosa*.

Declaration of competing interest

Acknowledgement

Appendix A. Supplementary data

Supplementary data to this article can be found online at https://doi.org/10.1016/j.micinf.2022.105017.

References

[1] Fischbach MA, Walsh CT. Antibiotics for emerging pathogens. Science 2009;325(80):1089−93. https://doi.org/10.1126/science.1176667.

[2] Williams P, Cámara M. Quorum sensing and environmental adaptation in Pseudomonas aeruginosa: a tale of regulatory networks and multifunctional signal molecules. Curr Opin Microbiol 2009;12:182−91. https://doi.org/10.1016/j.mib.2009.01.005.

[3] Pang Z, Raudonis R, Glick BR, Lin TJ, Cheng Z. Antibiotic resistance in Pseudomonas aeruginosa: mechanisms and alternative therapeutic strategies. Biotechnol Adv 2019;37:177−92. https://doi.org/10.1016/j.biotechadv.2018.11.013.

[4] Wallace DF. The regulation of iron absorption and homeostasis. Clin Biochem Rev 2016;37:51−62.

[5] Minandri F, Imperi F, Frangipani E, Bonchi C, Visaggio D, Facchini M, et al. Role of iron uptake systems in pseudomonas aeruginosa virulence and airway infection. Infect Immun 2016;84:2324−35. https://doi.org/10.1128/IAI.00098-16.

[6] Lister PD, Wolter DJ, Hanson ND. Antibacterial-resistant Pseudomonas aeruginosa: clinical impact and complex regulation of chromosomally encoded resistance mechanisms. Clin Microbiol Rev 2009;22:582. https://doi.org/10.1128/CMR.00040-09.

[7] Cox CD, Adams P. Siderophore activity of pyoverdin for Pseudomonas aeruginosa. Infect Immun 1985;48:130−8. https://doi.org/10.1128/iai.48.1.130-138.1985.

[8] Konings AF, Martin LW, Sharples KJ, Roddam LF, Latham R, Reid DW, et al. Pseudomonas aeruginosa uses multiple pathways to acquire iron during chronic infection in cystic fibrosis lungs. Infect Immun 2013;81:2697−704. https://doi.org/10.1128/IAI.00418-13.

[9] Yeterian E, Martin LW, Guillon L, Journet L, Lamont IL, Schalk IJ. Synthesis of the siderophore pyoverdine in Pseudomonas aeruginosa involves a periplasmic maturation. Amino Acids 2010;38:1447−59. https://doi.org/10.1007/S00726-009-0358-0.

[10] Visca P, Imperi F, Lamont IL. Pyoverdine siderophores: from biogenesis to biosignificance. Trends Microbiol 2006;15:22−30. https://doi.org/10.1016/j.tim.2006.11.004.

[11] Ringel MT, Dräger G, Brüser T. PvdO is required for the oxidation of dihydropyoverdine as the last step of fluorophore formation in Pseudomonas fluorescens. J Biol Chem 2018;293:2330−41. https://doi.org/10.1074/jbc.RA117.000121.

[12] Ringel MT, Dräger G, Brüser T. PvdN enzyme catalyzes a periplasmic pyoverdine modification. J Biol Chem 2016;291:23929−38. https://doi.org/10.1074/jbc.M116.755611.

[13] Ringel MT, Dräger G, Brüser T. The periplasmic transaminase PtaA of Pseudomonas fluorescens converts the glutamic acid residue at the pyoverdine fluorophore to -ketoglutaric acid. J Biol Chem 2017;292:18660−71. https://doi.org/10.1074/jbc.M117.812545.

[14] Tostado-Islas O, Mendoza-Ortiz A, Ramírez-García G, Cabrera-Takane ID, Loarca D, Pérez-González C, et al. Iron limitation by transferrin promotes simultaneous cheating of pyoverdine and exoprotease in Pseudomonas aeruginosa. ISME J 2021;15:2379−89. https://doi.org/10.1038/s41396-021-00938-6.

[15] Jimenez PN, Koch G, Papaioannou E, Wahjudi M, Krzeslak J, Coenye T, et al. Role of PvdQ in Pseudomonas aeruginosa virulence under iron-limiting conditions. Microbiology 2010;156:49−59. https://doi.org/10.1099/mic.0.030973-0.

[16] Clevenger KD, Wu R, Liu D, Fast W. n-Alkylboronic acid inhibitors reveal determinants of ligand specificity in the quorum-quenching and siderophore biosynthetic enzyme PvdQ. Biochemistry 2014;53:6679−86. https://doi.org/10.1021/bi501086s.

[17] Wurst JM, Drake EJ, Theriault JR, Jewett IT, Verplank L, Perez JR, et al. Identification of inhibitors of PvdQ, an enzyme involved in the synthesis of the siderophore pyoverdine. ACS Chem Biol 2014;9:1536−44. https://doi.org/10.1021/cb5001586.

[18] Bokhove M, Nadal Jimenez P, Quax WJ, Dijkstra BW. The quorum-quenching N-acyl homoserine lactone acylase PvdQ is an Ntn-hydrolase with an unusual substrate-binding pocket. Proc Natl Acad Sci U S A 2010;107:686−91. https://doi.org/10.1073/pnas.0911839107.

[19] Drake EJ, Gulick AM. Structural characterization and high-throughput screening of inhibitors of PvdQ, an NTN hydrolase involved in pyoverdine synthesis. ACS Chem Biol 2011;6:1277−86. https://doi.org/10.1021/cb2002973.

[20] Hanwell MD, Curtis DE, Lonie DC, Vandermeersch T, Zurek E, Hutchison GR. Avogadro: an advanced semantic chemical editor, visualization, and analysis platform. J Cheminf 2012;4:1−17.

[21] Trott O, Olson AJ. AutoDock Vina: improving the speed and accuracy of docking with a new scoring function, efficient optimization, and multithreading. J Comput Chem 2010;31:455−61. https://doi.org/10.1002/jcc.21334.

[22] Pettersen EF, Goddard TD, Huang CC, Couch GS, Greenblatt DM, Meng EC, et al. UCSF Chimera - a visualization system for exploratory research and analysis. J Comput Chem 2004;25:1605−12. https://doi.org/10.1002/jcc.20084.

[23] The PyMOL Molecular Graphics System. Version 1.20 schrodinger. LLC; 2012.

[24] Laskowski RA, Swindells MB. LigPlot+: multiple ligand−protein interaction diagrams for drug discovery. J Chem Inf Model 2011;51:2778−86. https://doi.org/10.1021/ci200227u.

[25] Rosati O, Curini M, Marcotullio MC, Oball-Mond G, Pelucchini C, Procopio A. Synthesis of 5-Amino-1,10b-dihydro-2 H-chromeno[3,4-c]pyridine-2,4(3 H)-diones from coumarins and cyanoacetamides under basic conditions. Synthesis 2010;4:239−48. https://doi.org/10.1055/s-0029-1217128.

[26] Clevenger KD, Wu R, Er JAV, Liu D, Fast W. Rational design of a transition state analogue with picomolar affinity for Pseudomonas aeruginosa PvdQ, a siderophore biosynthetic enzyme. ACS Chem Biol 2013;8:2192−200. https://doi.org/10.1021/cb400345h.

[27] Kang D, Revtovich AV, Chen Q, Shah KN, Cannon CL, Kirienko NV. Pyoverdine-dependent virulence of Pseudomonas aeruginosa isolates from cystic fibrosis patients. Front Microbiol 2019;10. https://doi.org/10.3389/FMICB.2019.02048/FULL.

[28] Ramarao N, Nielsen-Leroux C, Lereclus D. The insect Galleria mellonella as a powerful infection model to investigate bacterial pathogenesis. J Vis Exp 2012:e4392. https://doi.org/10.3791/4392.

[29] Gerner RR, Nuccio SP, Raffatellu M. Iron at the host-microbe interface. Mol Aspect Med 2020;75:100895. https://doi.org/10.1016/J.MAM.2020.100895.

[30] Gill EE, Franco OL, Hancock REW. Antibiotic adjuvants: diverse strategies for controlling drug-resistant pathogens. Chem Biol Drug Des 2015;85:56−78. https://doi.org/10.1111/cbdd.12478.

[31] Clevenger KD, Mascarenhas R, Daniel C, Wu R, Kelleher NL, Drake EJ, et al. Substrate trapping in the siderophore tailoring enzyme PvdQ HHS public access author manuscript. ACS Chem Biol 2017;12:643−7. https://doi.org/10.1021/acschembio.7b00031.